Superior discretizations and AMG solvers for extremely anisotropic diffusion via hyperbolic operators

Ben Southworth, Golo Wimmer, Xianzhu Tang, Thomas Gregory

17 Oct. 2023

Los Alamos NATIONAL LABORATORY

National Nuclear Security Administration
Managed by Triad National Security, LLC for the U.S. Department of Energy's NNSA

Outline

Anisotropic diffusion

Evolution of temperature T in plasma, heat flux $\mathbf{q}$, forcing S:

$$\frac{\partial T}{\partial t} - \nabla \cdot (\kappa_{\|} \nabla_{\|} + \kappa_{\perp} \nabla_{\perp}) T = S,$$

$$\text{(Dirichlet BCs)} \qquad T|_{\partial\Omega} = T_{\mathrm{BC}},$$

where $\mathbf{b} = \mathbf{B}/|\mathbf{B}|$ is direction of mangetic field lines, and

$$\nabla_{\|}(\cdot) := \mathbf{b} \cdot \nabla(\cdot))\mathbf{b},$$

$$\nabla_{\perp} := \nabla - \nabla_{\|}.$$

Anisotropic diffusion

Evolution of temperature T in plasma, heat flux $\mathbf{q}$, forcing S:

$$\frac{\partial T}{\partial t} - \nabla \cdot (\kappa_{\|}\nabla_{\|} + \kappa_{\perp}\nabla_{\perp})T = S,$$

$$\text{(Dirichlet BCs)} \qquad T|_{\partial\Omega} = T_{\text{BC}},$$

where $\mathbf{b} = \mathbf{B}/|\mathbf{B}|$ is direction of mangetic field lines, and

$$\nabla_{\|}(\cdot) := \mathbf{b} \cdot \nabla(\cdot))\mathbf{b},$$

$$\nabla_{\perp} := \nabla - \nabla_{\|}.$$

Many ways to skin a PDE!

Anisotropic diffusion

Evolution of temperature T in plasma, heat flux $\mathbf{q}$, forcing S:

$$\frac{\partial T}{\partial t} - \nabla \cdot \mathbf{q} = S,$$
$$\mathbf{q} = \kappa_{\|} \nabla_{\|} T + \kappa_{\perp} \nabla_{\perp} T,$$

where $\mathbf{b} = \mathbf{B}/|\mathbf{B}|$ is direction of mangetic field lines, and

$$\nabla_{\|}(\cdot) := \mathbf{b} \cdot \nabla(\cdot))\mathbf{b},$$
$$\nabla_{\perp} := \nabla - \nabla_{\|}.$$

Anisotropic diffusion

Evolution of temperature T in plasma, heat flux $\mathbf{q}$, forcing S:

$$\frac{\partial T}{\partial t} - \nabla \cdot \mathbf{q} = S,$$
$$\mathbf{q} = \kappa_{\|} \nabla_{\|} T + \kappa_{\perp} \nabla_{\perp} T,$$

where $\mathbf{b} = \mathbf{B}/|\mathbf{B}|$ is direction of mangetic field lines, and

$$\nabla_{\|}(\cdot) := \mathbf{b} \cdot \nabla(\cdot))\mathbf{b},$$
$$\nabla_{\perp} := \nabla - \nabla_{\|}.$$

- In magnetic confinement fusion, expect $\frac{\kappa_{\|}}{\kappa_{\perp}} \sim 10^9 - 10^{10}$.
- Parabolic equation in nature, but for non-grid-aligned $\mathbf{b}$, both discretization accuracy and implicit solve are very hard.

Directional gradient formulation

Define purely anisotropic conductivity $\kappa_\Delta := \kappa_\| - \kappa_\perp$.

- Diffusion isotropic if $\kappa_\Delta = 0$,
- Predominately anisotropic if $\kappa_\Delta \gg \kappa_\perp$.

Heat flux can be written as

$$\mathbf{q} = \kappa_\Delta \nabla_\| T + \kappa_\perp \nabla T.$$

Use directional derivative $\mathbf{b} \cdot \nabla T$ as auxiliary variable, reformulate

$$\frac{\partial T}{\partial t} - \sqrt{\kappa_\Delta} \nabla \cdot (\mathbf{b}\zeta) - \nabla \cdot (\kappa_\perp \nabla T) = S,$$

$$\zeta = \sqrt{\kappa_\Delta} \mathbf{b} \cdot \nabla T.$$

The steady state limit

Written in block operator form, directional gradient formulation is

$$\begin{pmatrix} \frac{\partial}{\partial t} + \kappa_\perp \Delta & -\sqrt{\kappa_\Delta}\nabla \cdot \left(\mathbf{b}(\cdot)\right) \\ -\sqrt{\kappa_\Delta}\mathbf{b} \cdot \nabla & I \end{pmatrix} \begin{pmatrix} T \\ \zeta \end{pmatrix} = \begin{pmatrix} S \\ 0 \end{pmatrix}.$$

The steady state limit

Written in block operator form, directional gradient formulation is

$$\begin{pmatrix} \frac{\partial}{\partial t} + \kappa_\perp \Delta & -\sqrt{\kappa_\Delta}\nabla \cdot \left(\mathbf{b}(\cdot)\right) \\ -\sqrt{\kappa_\Delta}\mathbf{b} \cdot \nabla & I \end{pmatrix} \begin{pmatrix} T \\ \zeta \end{pmatrix} = \begin{pmatrix} S \\ 0 \end{pmatrix}.$$

Consider steady-state (no time derivative) and purely anisotropic problem ($\kappa_\perp = 0$). Rearranging system, we have

$$\begin{pmatrix} -\sqrt{\kappa_\Delta}\mathbf{b} \cdot \nabla & I \\ \mathbf{0} & -\sqrt{\kappa_\Delta}\nabla \cdot \left(\mathbf{b}(\cdot)\right) \end{pmatrix} \begin{pmatrix} T \\ \zeta \end{pmatrix} = \begin{pmatrix} \mathbf{0} \\ S \end{pmatrix}.$$

The steady state limit

Written in block operator form, directional gradient formulation is

$$\begin{pmatrix} \frac{\partial}{\partial t} + \kappa_\perp \Delta & -\sqrt{\kappa_\Delta}\nabla \cdot (\mathbf{b}(\cdot)) \\ -\sqrt{\kappa_\Delta}\mathbf{b} \cdot \nabla & I \end{pmatrix} \begin{pmatrix} T \\ \zeta \end{pmatrix} = \begin{pmatrix} S \\ 0 \end{pmatrix}.$$

Consider steady-state (no time derivative) and purely anisotropic problem ($\kappa_\perp = 0$). Rearranging system, we have

$$\begin{pmatrix} -\sqrt{\kappa_\Delta}\mathbf{b} \cdot \nabla & I \\ \mathbf{0} & -\sqrt{\kappa_\Delta}\nabla \cdot (\mathbf{b}(\cdot)) \end{pmatrix} \begin{pmatrix} T \\ \zeta \end{pmatrix} = \begin{pmatrix} \mathbf{0} \\ S \end{pmatrix}.$$

$\Longrightarrow$ In the regime of extreme anisotropy, I claim we should treat this equation as a system of coupled hyperbolic operators rather than a parabolic operator.

Table of Contents

Upwind DG discretization

Discretize the transport term $\nabla \cdot \left(\sqrt{\kappa_\Delta}\mathbf{b}(\cdot)\right)$, using classical DG-upwind method:

$$L_b(\theta;\phi) := -\langle\sqrt{\kappa_\Delta}\theta\mathbf{b}, \nabla\phi\rangle + \int_\Gamma [\![\sqrt{\kappa_\Delta}\phi\mathbf{b}\cdot\mathbf{n}]\!]\tilde{\theta}\,\mathrm{d}S + \int_{\partial\Omega_{\text{out}}} \sqrt{\kappa_\Delta}\phi\mathbf{b}\cdot\mathbf{n}\theta\,\mathrm{d}S,$$

for L^2-inner product $\langle\cdot,\cdot\rangle$, and any functions $\theta, \phi \in \mathbb{V}_k^{\mathrm{DG}}(\Omega)$. $\partial\Omega_{\text{out}}$ denotes the outflow subset of boundary $\partial\Omega$ relative to $\mathbf{B}$, Γ denotes all interior facets, and

$$[\![\psi]\!] := \psi^+ - \psi^-, \qquad \tilde{\psi} := \begin{cases} \psi^+ & \text{if } \mathbf{b}^+\cdot\mathbf{n}^+ < 0, \\ \psi^- & \text{otherwise.} \end{cases}$$

Full weak form

Define two transport operators

$$L_{b,T}(\zeta_h;\phi) := L_b(\zeta_h;\phi) + \int_{\partial\Omega_{\text{in}}} \sqrt{\kappa_\Delta}\,\phi(\mathbf{b}\cdot\mathbf{n})\zeta_{\text{in}}\,\mathrm{d}S \qquad \forall\phi \in \mathbb{V}_k^{\text{DG}},$$

$$L_{b,\zeta}(\psi;T_h) := L_b(\psi;T_h) - \int_{\partial\Omega_{\text{out}}} \sqrt{\kappa_\Delta}\,T_{\text{BC}}(\mathbf{b}\cdot\mathbf{n})\psi\,\mathrm{d}S \quad \forall\psi \in \mathbb{V}_k^{\text{DG}},$$

where $\partial\Omega_{\text{in}}$ denotes inflow boundary, ζ_{in} is known.

$\Longrightarrow$ *Known inflow boundary ensure $L_{b,T}$, $L_{b,\zeta}$ are invertible*

Full weak form

Define two transport operators

$$L_{b,T}(\zeta_h;\phi) := L_b(\zeta_h;\phi) + \int_{\partial\Omega_{\text{in}}} \sqrt{\kappa_\Delta}\phi(\mathbf{b}\cdot\mathbf{n})\zeta_{\text{in}}\,\mathrm{d}S \qquad \forall\phi\in\mathbb{V}_k^{\text{DG}},$$

$$L_{b,\zeta}(\psi;T_h) := L_b(\psi;T_h) - \int_{\partial\Omega_{\text{out}}} \sqrt{\kappa_\Delta}T_{\text{BC}}(\mathbf{b}\cdot\mathbf{n})\psi\,\mathrm{d}S \quad \forall\psi\in\mathbb{V}_k^{\text{DG}},$$

where $\partial\Omega_{\text{in}}$ denotes inflow boundary, ζ_{in} is known.

$\implies$ *Known inflow boundary ensure $L_{b,T}$, $L_{b,\zeta}$ are invertible*

Two options for ζ_{in}:

1. Iterate implicit solve until $\zeta_{\text{in}} = \zeta_h$ (within nonlinear iteration for T, this is almost certainly less stiff and easier to resolve)
2. Treat auxiliary inflow ζ_{in} explicitly; so far have found in tests it varies slowly in time.

Full weak form

Define two transport operators

$$L_{b,T}(\zeta_h;\phi) := L_b(\zeta_h;\phi) + \int_{\partial\Omega_{\text{in}}} \sqrt{\kappa_\Delta}\,\phi(\mathbf{b}\cdot\mathbf{n})\zeta_{\text{in}}\,\mathrm{d}S \qquad \forall \phi \in \mathbb{V}_k^{\text{DG}},$$

$$L_{b,\zeta}(\psi;T_h) := L_b(\psi;T_h) - \int_{\partial\Omega_{\text{out}}} \sqrt{\kappa_\Delta}\,T_{\text{BC}}(\mathbf{b}\cdot\mathbf{n})\psi\,\mathrm{d}S \quad \forall \psi \in \mathbb{V}_k^{\text{DG}},$$

where $\partial\Omega_{\text{in}}$ denotes inflow boundary, ζ_{in} is known.

Weak form: find $(T_h, \zeta_h) \in (\mathbb{V}_k^{\text{DG}} \times \mathbb{V}_k^{\text{DG}})$ such that

$$\left\langle \phi, \frac{\partial T_h}{\partial t} \right\rangle - L_{b,T}(\zeta_h;\phi) - \text{IP}(T_h;\phi) = -\int_{\partial\Omega} \kappa_{\text{BC}}\phi(T_h - T_{\text{BC}})\,\mathrm{d}S + \langle \phi, S\rangle,$$

$$\langle \psi, \zeta_h \rangle + L_{b,\zeta}(\psi;T_h) = 0 \qquad \forall \psi,\phi \in \mathbb{V}_k^{\text{DG}}.$$

MHD test problem

Domain $\Omega = [0,1] \times [0,1] \times [0,5]$, periodic in z, initial T

$$T_0 = \sin\left(\frac{\pi x}{L_x}\right) \sin\left(\frac{\pi y}{L_x}\right),$$

with $T_{\text{BC}} = 0$ on $\partial\Omega$. **B** aligns with contours of T_0 in (x, y) and is constant in z,

$$\mathbf{B} = (B_x, B_y, B_z) = (-\partial_y T, \partial_x T, 5)$$

$\implies$ ensures $(B_x, B_y) = \nabla^{\perp} T_0$ for 2D curl $\nabla^{\perp} = (-\partial_y, \partial_x)$.

MHD test problem

Domain $\Omega = [0,1] \times [0,1] \times [0,5]$, periodic in z, initial T

$$T_0 = \sin\left(\frac{\pi x}{L_x}\right) \sin\left(\frac{\pi y}{L_x}\right),$$

with $T_{\mathrm{BC}} = 0$ on $\partial\Omega$. **B** aligns with contours of T_0 in (x, y) and is constant in z,

$$\mathbf{B} = (B_x, B_y, B_z) = (-\partial_y T, \partial_x T, 5)$$

$\implies$ ensures $(B_x, B_y) = \nabla^\perp T_0$ for 2D curl $\nabla^\perp = (-\partial_y, \partial_x)$.

Add counter forcing $S = -\kappa_\perp \Delta T_0$, to ensure a steady state test case. Error can be measured relative to the initial condition,

$$e_T(t) = \frac{\| T_h(t) - T_0 \|_2}{\| T_0 \|_2}.$$

Accuracy and results

Compare with:

- **CG-primal system:** (i.e. without auxiliary heat flux) for T in second order CG, $\mathbb{V}_2^{\mathrm{CG}}$.
- **DG-primal system:** for T in $\mathbb{V}_2^{\mathrm{DG}}$ (similar to recent papers Green et al, Vogl et al.).
- **Mixed CG:** original directional gradient formulation in $\mathbb{V}_2^{\mathrm{CG}}$-$\mathbb{V}_1^{\mathrm{DG}}$ from Gunter et al (does not use transport disc. techniques).

Accuracy and results

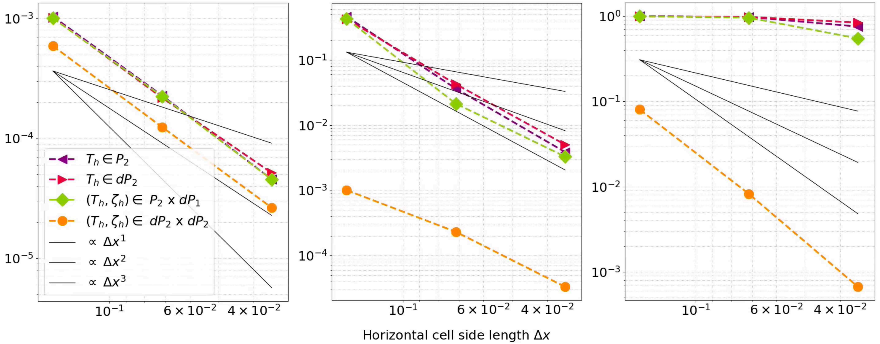

Figure: Relative L^2 error for anisotropy ratios from left to right 10^3, 10^6, and 10^9. Orange circles denote novel mixed DG scheme, green diamonds mixed CG, red triangles primal DG, and purple triangles primal CG.

Table of Contents

Continuous Galerkin

Let $\mathbb{V}_T := CG(\Omega)_k$ denote kth order continuous Galerkin space, and

$$\mathbb{V}_{T_{bc}} := \{\eta \in CG(\Omega)_k \colon \eta|_{\partial\Omega} = T_{bc}\}, \quad \mathring{\mathbb{V}}_T := \{\eta \in CG(\Omega)_k \colon \eta|_{\partial\Omega} = 0\}.$$

Weak form: find $(T \in \mathbb{V}_{T_{bc}},\ \zeta \in \mathbb{V}_\zeta)$ such that

$$\left\langle \eta, \frac{\partial T}{\partial t} \right\rangle + \langle \kappa_\| \mathbf{b} \cdot \nabla \eta, \zeta \rangle = F \qquad \forall \eta \in \mathring{\mathbb{V}}_T, \qquad (1)$$

$$\langle \eta, \zeta - \mathbf{b} \cdot \nabla T \rangle = 0 \qquad \forall \phi \in \mathbb{V}_\zeta. \qquad (2)$$

for CG or DG auxiliary space $\mathbb{V}_\zeta$ w/o any associated BCs.

- Analogous to DG case, we set auxilliary space equal to temperature space (ensures square advective blocks).

Transport stabilization (it works!)

Define velocity field $\mathbf{s} := \sqrt{\kappa_{\|}}\mathbf{b}$. For stabilization parameter τ, define advective and flux based SUPG operators

$$S_a(\eta) = \eta + \tau\mathbf{s}\cdot\nabla\eta, \qquad S_f(\eta) = \eta + \mathbf{s}\cdot\nabla(\tau\eta).$$

Mixed CG, SUPG stabilized discretization given by

$$\begin{aligned}\left\langle S_a(\eta), \frac{\partial T}{\partial t}\right\rangle + \langle \mathbf{s}\cdot\nabla\eta, S_f(\zeta)\rangle = \langle S_a(\eta), F\rangle + \\ \int_{\partial\Omega} \tau(\mathbf{s}\cdot\nabla\eta)(\mathbf{s}\cdot\mathbf{n})(\mathbf{s}\cdot\nabla T)dS \qquad & \forall \eta \in \mathring{\mathbb{V}}_T, \\ \langle \eta, S_f(\zeta)\rangle - \langle \mathbf{s}\cdot\nabla T, S_f(\eta)\rangle = 0 \qquad & \forall \eta \in \mathbb{V}_T.\end{aligned}$$

for temperature $T \in \mathbb{V}_{T_{bc}}$ and auxiliary variable $\zeta \in \mathbb{V}_T$.

Transport stabilization (it works!)

- A boundary integral appears because while η vanishes along Dirichlet boundary, SUPG-modification $\mathbf{s} \cdot \nabla \eta$ need not (gradient first computed within cells neighboring $\partial\Omega$, then evaluated along $\partial\Omega$)
- Averaged stabilization parameter for tuning parameter $\lambda \in [0, 1]$:

$$\tau = \left(\lambda \frac{2}{\Delta t} + \frac{\sqrt{\kappa_\parallel}}{2\Delta x} \right)^{-1}$$

- Specific form of $S_f(\eta)$ and $S_a(\eta)$ derived for structure preservation and consistency.
- In practice, we use weak BCs for CG formulation. Recall we swap the algebraic system's block rows. In Firedrake, non-trivial to form the correct block row-swapped system with strong BCs.

Accuracy (quads)

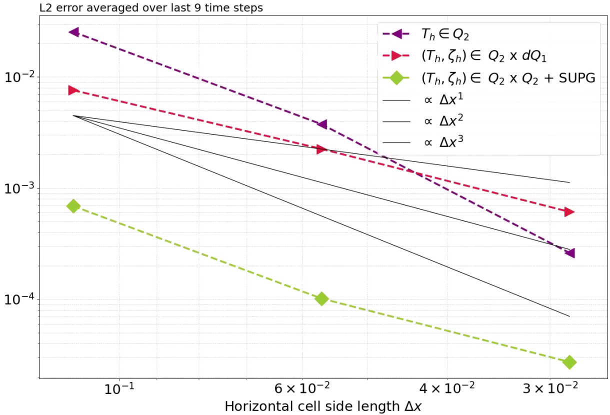

Figure: Magnetic surface test case: plasma trapped in series of concentric tori. We "unfold" concentric tori with rational winding number and temperature perturbation spreading on surface. $\kappa_\perp = 0, \kappa_\| = 100$, integrate to one Alfven time.

Accuracy (triangles)

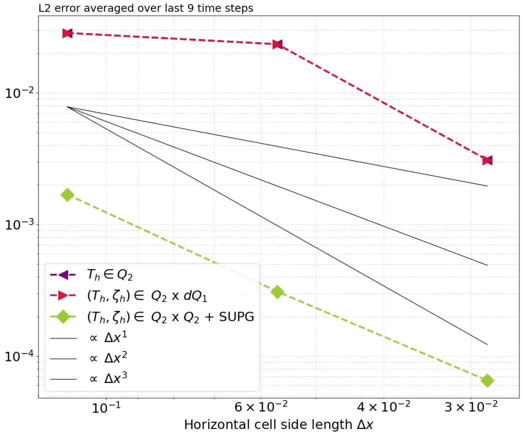

Figure: Magnetic surface test case; “unfolded” concentric tori with rational winding number and temperature perturbation spreading on surface. $\kappa_\perp = 0, \kappa_{||} = 100$, integrate to one Alfven time.

Table of Contents

Consistency

Proposition: *The CG and DG space discretizations are consistent, i.e. a solution satisfying the continuous equation also satisfies the discretizations with sufficiently regular test functions* η*.*

Note, most discretizations would be consistent, but using stabilization techniques like hyper-diffusion are not.

Diffusion

Continuous system is dissipative up to up to forcing and total in- and outflux:

$$\frac{1}{2}\frac{d}{dt}\|T\|_2^2 = \langle T, F\rangle - \|\sqrt{\kappa_\|}\mathbf{b}\cdot\nabla T\|_2^2 + \int_{\partial\Omega} T\kappa_\|(\mathbf{b}\cdot\mathbf{n})(\mathbf{b}\cdot\nabla T)dS.$$

- DG discretization satisfies this weakly, in the sense that the diffusion property is satisfied up to a weak BC penalty, and if a strong solution satisfies the BCs, we satisfy the diffusion property.
- CG discretization with Neumann or weak Dirichlet BCs satisfies this weakly.

Energy/Temperature

Continuous system conserves total temperature up to forcing and total in- and outflux:

$$\frac{d}{dt}\int_{\Omega} T\ dx = \int_{\Omega} F\ dx + \int_{\partial\Omega} \kappa_{\|}(\mathbf{b}\cdot\mathbf{n})(\mathbf{b}\cdot\nabla T)dS.$$

- DG discretization satisfies this weakly up to normal continuity **b** (strong solution will satisfy).
- CG discretization with Neumann BCs satisfies this automatically.
- CG discretization with weak Dirichlet BCs satisfies this weakly (multiple extra terms in weak form, but eliminated with strong solution).

Spurious heat loss

Movie!

Spurious heat loss

- $\kappa_\perp = 0$, physical $\kappa_\|$ taken from Braginski model, fixed Dirichlet BCs.
- Time step of 1 Alfven time.
- Periodic domain in angle, CG disc. has 11K DOFs, DG disc. 47K DOFs.

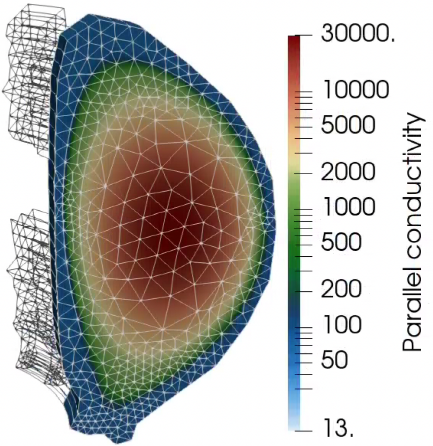

Spurious heat loss

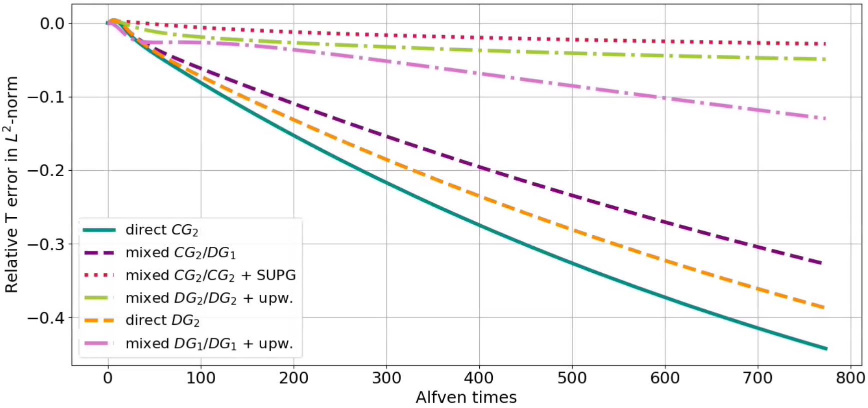

Figure: Spurious temperature loss for different discretizations. Final losses: CG2: -44%; DG2: -39%; CG2-DG1: -33%; DG1-DG1: -13%; DG2-DG2: -4.9%; CG2-CG2: -2.8%.

Table of Contents

Algebraic multigrid (AMG)

One of fastest methods (when applicable) to solve large, sparse systems $A\mathbf{x} = \mathbf{b}$.

$\Longrightarrow$ Two parts: *Relaxation* and *coarse-grid correction*:

$$\mathbf{x}_{k+1} = \mathbf{x}_k + M^{-1}(\mathbf{b} - A\mathbf{x}_k),$$
$$\mathbf{x}_{k+1} = \mathbf{x}_k + P(RAP)^{-1}R(\mathbf{b} - A\mathbf{x}_k).$$

Algebraic multigrid (AMG)

One of fastest methods (when applicable) to solve large, sparse systems $A\mathbf{x} = \mathbf{b}$.

$\implies$ Two parts: *Relaxation* and *coarse-grid correction*:

$$\mathbf{e}_{k+1} = (I - M^{-1}A)\mathbf{e}_k,$$

$$\begin{aligned}\mathbf{e}_{k+1} &= (I - P(RAP)^{-1}RA)\mathbf{e}_k \\ &= (I - \Pi)\mathbf{e}_k.\end{aligned}$$

Algebraic multigrid (AMG)

One of fastest methods (when applicable) to solve large, sparse systems $A\mathbf{x} = \mathbf{b}$.

$\implies$ Two parts: *Relaxation* and *coarse-grid correction*:

$$\mathbf{e}_{k+1} = (I - M^{-1}A)\mathbf{e}_k,$$

$$\begin{aligned}\mathbf{e}_{k+1} &= (I - P(RAP)^{-1}RA)\mathbf{e}_k \\ &= (I - \Pi)\mathbf{e}_k.\end{aligned}$$

AMG is typically for symmetric positive definite (SPD) matrices.

- If A is SPD, $\|\mathbf{x}\|_A^2 = \langle A\mathbf{x}, \mathbf{x}\rangle$ defines norm.
- $R := P^T \implies \|\Pi\|_A = 1$.

Algebraic multigrid (AMG)

One of fastest methods (when applicable) to solve large, sparse systems $A\mathbf{x} = \mathbf{b}$.

$\implies$ Two parts: *Relaxation* and *coarse-grid correction*:

$$\mathbf{e}_{k+1} = (I - M^{-1}A)\mathbf{e}_k,$$
$$\mathbf{e}_{k+1} = (I - P(RAP)^{-1}RA)\mathbf{e}_k$$
$$= (I - \Pi)\mathbf{e}_k.$$

AMG is typically for symmetric positive definite (SPD) matrices.

- If A is SPD, $\|\mathbf{x}\|_A^2 = \langle A\mathbf{x}, \mathbf{x}\rangle$ defines norm.
- $R := P^T \implies \|\Pi\|_A = 1$.
- **Non-orthogonal projection can increase error ☹**

Notation

CF-Splitting:

- Assume DOFs partitioned into coarse points (C) and fine points (F)

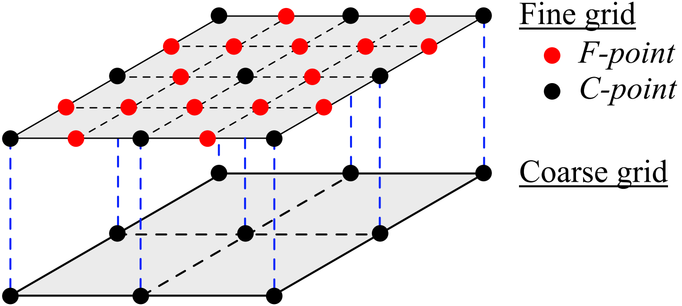

Notation

CF-Splitting:

- Assume DOFs partitioned into coarse points (C) and fine points (F)

Write vectors and matrices in block form:

$$
A = \begin{pmatrix} A_{ff} & A_{fc} \\ A_{cf} & A_{cc} \end{pmatrix}, \qquad P = \begin{pmatrix} W \\ I \end{pmatrix},
$$
$$
R = \begin{pmatrix} Z & I \end{pmatrix}, \qquad \mathcal{K} := RAP.
$$

Coarse-grid correction and R_{ideal}

Decompose F-point error $\mathbf{e}_f = W\mathbf{e}_c + \delta\mathbf{e}_f$:

$$\mathbf{e}^{(i+1)} = \begin{pmatrix} \mathbf{e}_f^{(i)} \\ \mathbf{e}_c^{(i)} \end{pmatrix} - P(RAP)^{-1}RA\left[\begin{pmatrix} W\mathbf{e}_c^{(i)} \\ \mathbf{e}_c^{(i)} \end{pmatrix} + \begin{pmatrix} \delta\mathbf{e}_f^{(i)} \\ \mathbf{0} \end{pmatrix}\right]$$

Coarse-grid correction and R_{ideal}

Decompose F-point error $\mathbf{e}_f = W\mathbf{e}_c + \delta\mathbf{e}_f$:

$$\mathbf{e}^{(i+1)} = \begin{pmatrix} \mathbf{e}_f^{(i)} \\ \mathbf{e}_c^{(i)} \end{pmatrix} - P(RAP)^{-1}RA\left[\begin{pmatrix} W\mathbf{e}_c^{(i)} \\ \mathbf{e}_c^{(i)} \end{pmatrix} + \begin{pmatrix} \delta\mathbf{e}_f^{(i)} \\ \mathbf{0} \end{pmatrix}\right]$$

$$= \begin{pmatrix} \mathbf{e}_f^{(i)} - W\mathbf{e}_c^{(i)} \\ \mathbf{0} \end{pmatrix} - P(RAP)^{-1}RA\begin{pmatrix} \delta\mathbf{e}_f^{(i)} \\ \mathbf{0} \end{pmatrix}.$$

Coarse-grid correction and R_{ideal}

Decompose F-point error $\mathbf{e}_f = W\mathbf{e}_c + \delta\mathbf{e}_f$:

$$\mathbf{e}^{(i+1)} = \begin{pmatrix} \mathbf{e}_f^{(i)} \\ \mathbf{e}_c^{(i)} \end{pmatrix} - P(RAP)^{-1}RA\left[\begin{pmatrix} W\mathbf{e}_c^{(i)} \\ \mathbf{e}_c^{(i)} \end{pmatrix} + \begin{pmatrix} \delta\mathbf{e}_f^{(i)} \\ \mathbf{0} \end{pmatrix}\right]$$

$$= \begin{pmatrix} \mathbf{e}_f^{(i)} - W\mathbf{e}_c^{(i)} \\ \mathbf{0} \end{pmatrix} - P(RAP)^{-1}RA\begin{pmatrix} \delta\mathbf{e}_f^{(i)} \\ \mathbf{0} \end{pmatrix}.$$

Coarse-grid correction and R_{ideal}

Decompose F-point error $\mathbf{e}_f = W\mathbf{e}_c + \delta\mathbf{e}_f$:

$$\mathbf{e}^{(i+1)} = \begin{pmatrix} \mathbf{e}_f^{(i)} \\ \mathbf{e}_c^{(i)} \end{pmatrix} - P(RAP)^{-1}RA\left[\begin{pmatrix} W\mathbf{e}_c^{(i)} \\ \mathbf{e}_c^{(i)} \end{pmatrix} + \begin{pmatrix} \delta\mathbf{e}_f^{(i)} \\ \mathbf{0} \end{pmatrix}\right]$$

$$= \begin{pmatrix} \mathbf{e}_f^{(i)} - W\mathbf{e}_c^{(i)} \\ \mathbf{0} \end{pmatrix} - P(RAP)^{-1}RA\begin{pmatrix} \delta\mathbf{e}_f^{(i)} \\ \mathbf{0} \end{pmatrix}.$$

Ideal restriction:

$$RA\begin{pmatrix} \delta\mathbf{e}_f^{(i)} \\ \mathbf{0} \end{pmatrix} = (ZA_{ff} + A_{cf})\delta\mathbf{e}_f = \mathbf{0}$$

$$\implies \quad \underline{R_{\text{ideal}} = \begin{pmatrix} -A_{cf}A_{ff}^{-1} & I \end{pmatrix}}$$

Coarse-grid correction and R_{ideal}

Decompose F-point error $\mathbf{e}_f = W\mathbf{e}_c + \delta\mathbf{e}_f$:

$$\mathbf{e}^{(i+1)} = \begin{pmatrix} \mathbf{e}_f^{(i)} \\ \mathbf{e}_c^{(i)} \end{pmatrix} - P(RAP)^{-1}RA\left[\begin{pmatrix} W\mathbf{e}_c^{(i)} \\ \mathbf{e}_c^{(i)} \end{pmatrix} + \begin{pmatrix} \delta\mathbf{e}_f^{(i)} \\ \mathbf{0} \end{pmatrix}\right]$$
$$= \begin{pmatrix} \mathbf{e}_f^{(i)} - W\mathbf{e}_c^{(i)} \\ \mathbf{0} \end{pmatrix} - P(RAP)^{-1}RA\begin{pmatrix} \delta\mathbf{e}_f^{(i)} \\ \mathbf{0} \end{pmatrix}.$$

Lemma 1 (Orthogonal coarse-grid correction).
Coarse-grid correction with

$$R_{\text{ideal}} = \begin{pmatrix} -A_{cf}A_{ff}^{-1} & I \end{pmatrix}, \qquad P = \begin{pmatrix} \mathbf{0} \\ I \end{pmatrix}$$

is an ℓ^2-orthogonal projection.

Reduction based AMG as block LDU

Partition (discontinuous) elements into C-elements and F-elements. Then in matrix form,

$$\begin{bmatrix} A_{ff} & A_{fc} \\ A_{cf} & A_{cc} \end{bmatrix}^{-1} = \begin{bmatrix} I & -A_{ff}^{-1}A_{fc} \\ 0 & I \end{bmatrix} \begin{bmatrix} A_{ff}^{-1} & 0 \\ 0 & \mathcal{S}^{-1} \end{bmatrix} \begin{bmatrix} I & 0 \\ -A_{cf}A_{ff}^{-1} & I \end{bmatrix}.$$

Reduction based AMG preconditioner M^{-1} looks like:

$$M^{-1} = \begin{bmatrix} I & \widehat{W} \\ 0 & I \end{bmatrix} \begin{bmatrix} \Delta_F & 0 \\ 0 & \mathcal{K}^{-1} \end{bmatrix} \begin{bmatrix} I & 0 \\ Z & I \end{bmatrix},$$

where $\widehat{W} = (I - \Delta_F A_{ff})W - \Delta A_{fc}$. Want $\Delta_F \simeq A_{ff}^{-1}$, $Z \simeq -A_{cf}A_{ff}^{-1}$.

Reduction based AMG as block LDU

Partition (discontinuous) elements into C-elements and F-elements. Then in matrix form,

$$\begin{bmatrix} A_{ff} & A_{fc} \\ A_{cf} & A_{cc} \end{bmatrix}^{-1} = \begin{bmatrix} I & -A_{ff}^{-1}A_{fc} \\ 0 & I \end{bmatrix} \begin{bmatrix} A_{ff}^{-1} & 0 \\ 0 & \mathcal{S}^{-1} \end{bmatrix} \begin{bmatrix} I & 0 \\ -A_{cf}A_{ff}^{-1} & I \end{bmatrix}.$$

Reduction based AMG preconditioner M^{-1} looks like:

$$M^{-1} = \begin{bmatrix} I & \widehat{W} \\ 0 & I \end{bmatrix} \begin{bmatrix} \Delta_F & 0 \\ 0 & \mathcal{K}^{-1} \end{bmatrix} \begin{bmatrix} I & 0 \\ Z & I \end{bmatrix},$$

where $\widehat{W} = (I - \Delta_F A_{ff})W - \Delta A_{fc}$. Want $\Delta_F \simeq A_{ff}^{-1}$, $Z \simeq -A_{cf}A_{ff}^{-1}$.

$\Longrightarrow$ **Can we approximate A_{ff}^{-1} well?**

Approximate ideal restriction

For ith C-point (ith row of R), choose restriction neighborhood $\mathcal{R}_i = \{\ell_1, ..., \ell_{S_i}\}$ of some "nearby" F-points. Solve

$$a_{ij} + \sum_{k \in \mathcal{R}_i} z_{ik} a_{kj} = 0.$$

Sets RA equal to zero within F-point sparsity pattern.

Approximate ideal restriction

For ith C-point (ith row of R), choose restriction neighborhood $\mathcal{R}_i = \{\ell_1, ..., \ell_{S_i}\}$ of some "nearby" F-points. Solve

$$a_{ij} + \sum_{k \in \mathcal{R}_i} z_{ik} a_{kj} = 0.$$

Sets RA equal to zero within F-point sparsity pattern.

$$\begin{pmatrix} a_{\ell_0\ell_0} & a_{\ell_1\ell_0} & ... & a_{\ell_{S_i}\ell_0} \\ a_{\ell_0\ell_1} & a_{\ell_1\ell_1} & ... & a_{\ell_{S_i}\ell_1} \\ \vdots & & \ddots & \vdots \\ a_{\ell_0\ell_{S_i}} & a_{\ell_1\ell_{S_i}} & ... & a_{\ell_{S_i}\ell_{S_i}} \end{pmatrix} \begin{pmatrix} z_{i\ell_0} \\ z_{i\ell_1} \\ \vdots \\ z_{i\ell_{S_i}} \end{pmatrix} = - \begin{pmatrix} a_{i\ell_0} \\ a_{i\ell_1} \\ \vdots \\ a_{i\ell_{S_i}} \end{pmatrix}$$

Approximate ideal restriction

For ith C-point (ith row of R), choose restriction neighborhood $\mathcal{R}_i = \{\ell_1, ..., \ell_{S_i}\}$ of some "nearby" F-points. Solve

$$a_{ij} + \sum_{k \in \mathcal{R}_i} z_{ik} a_{kj} = 0.$$

Sets RA equal to zero within F-point sparsity pattern.

Goal:

1. Use AIR to achieve accurate solution at C-points.
2. Follow with F-relaxation to distribute accuracy to F-points.

AIR for upwind transport

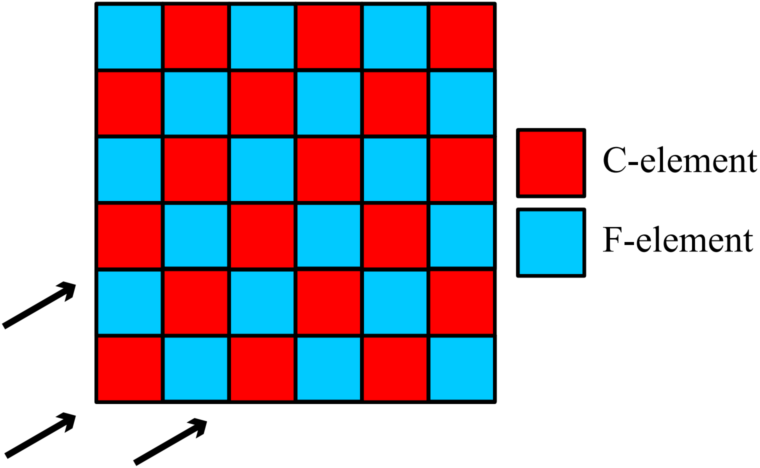

Consider transport on structured 2d grid and partition elements into C-elements and F-elements.

AIR for upwind transport

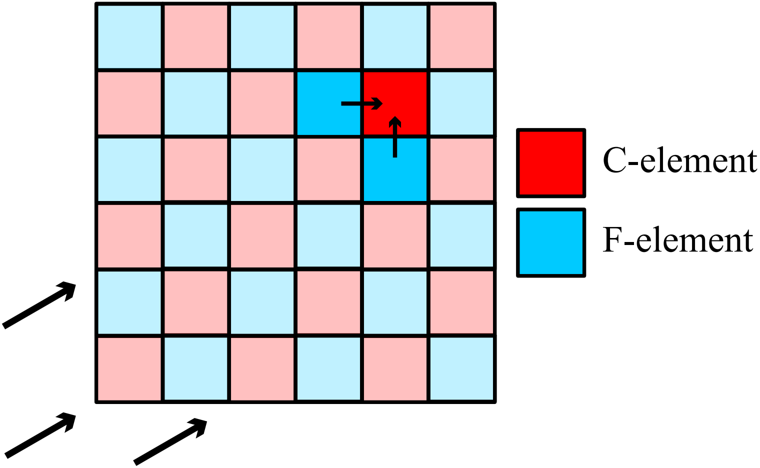

Notice that there are no C-C or F-F connections

$$\implies A_{ff} = A_{cc} = I.$$

AIR for upwind transport

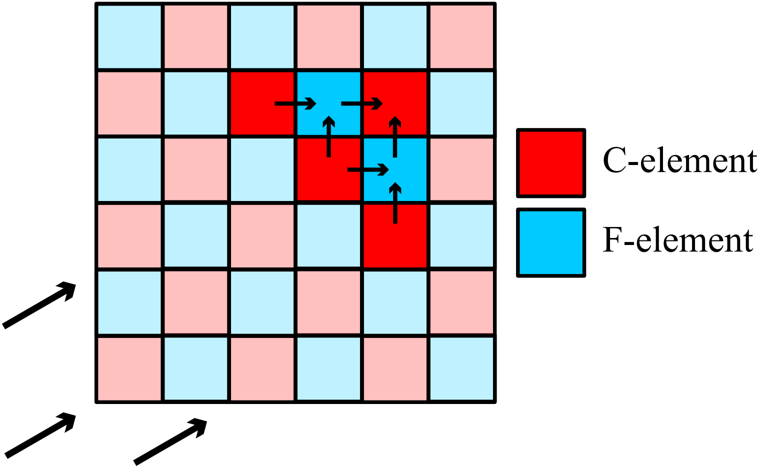

If $A_{ff} = I$, AMG coarse grid given by $A_{cc} - A_{cf}A_{fc} \iff$ all C-F-C connections.

AIR for upwind transport

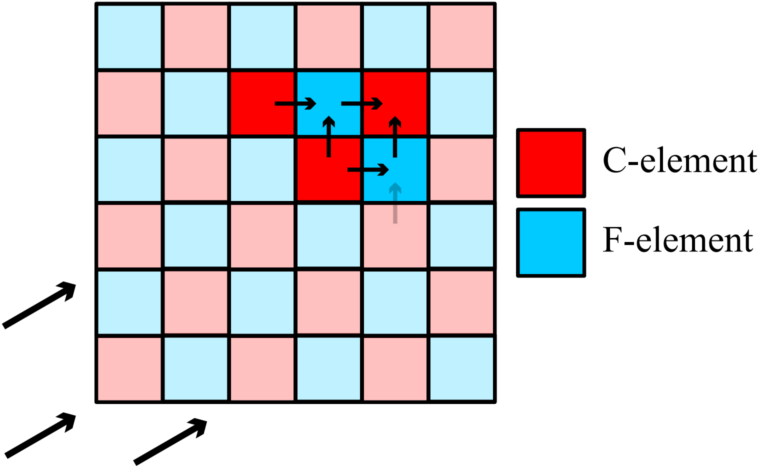

If $A_{ff} = I$, AMG coarse grid given by $A_{cc} - A_{cf}A_{fc} \iff$ all C-F-C connections. **One of these connections is weak!**

Table of Contents

2×2 DG system

Reorder discrete 2×2 block system

$$\begin{pmatrix} -\sqrt{\kappa_\Delta} G_b & M \\ \frac{1}{\Delta t}(M + \tilde{\kappa}_{\text{BC}} M_{\text{BC},h_e}) + \kappa_\perp L & \sqrt{\kappa_\Delta} G_b^T \end{pmatrix} \begin{pmatrix} T^{n+1} \\ \zeta^{n+1} \end{pmatrix} = \begin{pmatrix} F_\zeta \\ F_T \end{pmatrix}.$$

Assume $\tilde{\kappa}_{BC} \sim \mathcal{O}(1)$, so that $M + \tilde{\kappa}_{\text{BC}} M_{\text{BC},h_e} \approx M$ in spectral analysis. Apply block triangular preconditioner,

$$\begin{pmatrix} -\sqrt{\kappa_\Delta} G_b & \mathbf{0} \\ \frac{1}{\Delta t}(M + \tilde{\kappa}_{\text{BC}} M_{\text{BC}}) + \kappa_\perp L & \sqrt{\kappa_\Delta} G_b^T \end{pmatrix}^{-1}.$$

2×2 DG system

Reorder discrete 2×2 block system

$$\begin{pmatrix} -\sqrt{\kappa_\Delta} G_b & M \\ \frac{1}{\Delta t}(M + \tilde{\kappa}_{\text{BC}} M_{\text{BC},h_e}) + \kappa_\perp L & \sqrt{\kappa_\Delta} G_b^T \end{pmatrix} \begin{pmatrix} T^{n+1} \\ \zeta^{n+1} \end{pmatrix} = \begin{pmatrix} F_\zeta \\ F_T \end{pmatrix}.$$

Assume $\tilde{\kappa}_{BC} \sim \mathcal{O}(1)$, so that $M + \tilde{\kappa}_{\text{BC}} M_{\text{BC},h_e} \approx M$ in spectral analysis. Apply block triangular preconditioner,

$$\begin{pmatrix} -\sqrt{\kappa_\Delta} G_b & \mathbf{0} \\ \frac{1}{\Delta t}(M + \tilde{\kappa}_{\text{BC}} M_{\text{BC}}) + \kappa_\perp L & \sqrt{\kappa_\Delta} G_b^T \end{pmatrix}^{-1}.$$

Convergence of fixed-point / Krylov fully defined by approximating Schur complement:

$$S_{22} := \sqrt{\kappa_\Delta} G_b^T + \left(\frac{1}{\Delta t} M + \kappa_\perp L\right)\left(\sqrt{\kappa_\Delta} G_b\right)^{-1} M.$$

Spectral analysis of Schur complement

Preconditioned S_{22} similar to SPD operator:

$$
\begin{aligned}
(\sqrt{\kappa_\Delta} G_b^T)^{-1} S_{22} &= I + \tfrac{1}{\Delta t \kappa_\Delta} G_b^{-T} M G_b^{-1} M + \tfrac{\kappa_\perp}{\kappa_\Delta} G_b^{-T} L G_b^{-1} M \\
&\sim I + \tfrac{1}{\Delta t \kappa_\Delta} M^{1/2} G_b^{-T} M G_b^{-1} M^{1/2} + \tfrac{\kappa_\perp}{\kappa_\Delta} M^{1/2} G_b^{-T} L G_b^{-1} M^{1/2}.
\end{aligned}
$$

Spectral analysis of Schur complement

Preconditioned S_{22} similar to SPD operator:

$$
\begin{aligned}
(\sqrt{\kappa_\Delta} G_b^T)^{-1} S_{22} &= I + \frac{1}{\Delta t \kappa_\Delta} G_b^{-T} M G_b^{-1} M + \frac{\kappa_\perp}{\kappa_\Delta} G_b^{-T} L G_b^{-1} M \\
&\sim I + \frac{1}{\Delta t \kappa_\Delta} M^{1/2} G_b^{-T} M G_b^{-1} M^{1/2} + \frac{\kappa_\perp}{\kappa_\Delta} M^{1/2} G_b^{-T} L G_b^{-1} M^{1/2}.
\end{aligned}
$$

First (anisotropic) term: for mesh h and constants c_1, c_2:

$$
\sigma \left(\frac{1}{\Delta t \kappa_\Delta} M^{1/2} G_b^{-T} M G_b^{-1} M^{1/2} \right) \subset \frac{1}{\Delta t \kappa_\Delta} [c_1 h^2, c_2].
$$

Spectral analysis of Schur complement

Preconditioned S_{22} similar to SPD operator:

$$\begin{aligned}(\sqrt{\kappa_\Delta} G_b^T)^{-1} S_{22} &= I + \frac{1}{\Delta t \kappa_\Delta} G_b^{-T} M G_b^{-1} M + \frac{\kappa_\perp}{\kappa_\Delta} G_b^{-T} L G_b^{-1} M \\ &\sim I + \frac{1}{\Delta t \kappa_\Delta} M^{1/2} G_b^{-T} M G_b^{-1} M^{1/2} + \frac{\kappa_\perp}{\kappa_\Delta} M^{1/2} G_b^{-T} L G_b^{-1} M^{1/2}.\end{aligned}$$

First (anisotropic) term: for mesh h and constants c_1, c_2:

$$\sigma\left(\frac{1}{\Delta t \kappa_\Delta} M^{1/2} G_b^{-T} M G_b^{-1} M^{1/2}\right) \subset \frac{1}{\Delta t \kappa_\Delta}[c_1 h^2, c_2].$$

Second (isotropic) term: 2D and **b** aligned in x. Second term $\sim \partial_{xx}^{-1}(\partial_{xx} + \partial_{yy}) = 1 + \partial_{xx}^{-1}\partial_{yy}$. On unit domain, Laplacian eigendecomposition $\{u_{jk}, \pi^2(j^2 + k^2)\}$, $u_{jk} = 2\sin(j\pi x)\sin(k\pi y)$; similar for ∂_{xx} in (j, x). $\implies$ Highest frequency in y, $k = 1/h$, and smoothest in x, $j = 1$, yields eigenpair

$$(1 + \partial_{xx}^{-1}\partial_{yy}) 2\sin(\pi x)\sin(\tfrac{1}{h}\pi y) = \left(1 + \tfrac{1}{h^2}\right) 2\sin(\pi x)\sin(\tfrac{1}{h}\pi y).$$

Spectral analysis of Schur complement

Preconditioned S_{22} similar to SPD operator:

$$(\sqrt{\kappa_\Delta} G_b^T)^{-1} S_{22} = I + \frac{1}{\Delta t \kappa_\Delta} G_b^{-T} M G_b^{-1} M + \frac{\kappa_\perp}{\kappa_\Delta} G_b^{-T} L G_b^{-1} M$$
$$\sim I + \frac{1}{\Delta t \kappa_\Delta} M^{1/2} G_b^{-T} M G_b^{-1} M^{1/2} + \frac{\kappa_\perp}{\kappa_\Delta} M^{1/2} G_b^{-T} L G_b^{-1} M^{1/2}.$$

First (anisotropic) term: for mesh h and constants c_1, c_2:

$$\sigma\left(\frac{1}{\Delta t \kappa_\Delta} M^{1/2} G_b^{-T} M G_b^{-1} M^{1/2}\right) \subset \frac{1}{\Delta t \kappa_\Delta}[c_1 h^2, c_2].$$

Second (isotropic) term:

$$\sigma\left(\frac{\kappa_\perp}{\kappa_\Delta} M^{1/2} G_b^{-T} L G_b^{-1} M^{1/2}\right) \subset \left(0, \frac{\kappa_\perp c_3}{\kappa_\Delta h^2}\right],$$

Spectral analysis of Schur complement

Preconditioned S_{22} similar to SPD operator:

$$(\sqrt{\kappa_\Delta} G_b^T)^{-1} S_{22} = I + \frac{1}{\Delta t \kappa_\Delta} G_b^{-T} M G_b^{-1} M + \frac{\kappa_\perp}{\kappa_\Delta} G_b^{-T} L G_b^{-1} M$$

$$\sim I + \frac{1}{\Delta t \kappa_\Delta} M^{1/2} G_b^{-T} M G_b^{-1} M^{1/2} + \frac{\kappa_\perp}{\kappa_\Delta} M^{1/2} G_b^{-T} L G_b^{-1} M^{1/2}.$$

First (anisotropic) term: for mesh h and constants c_1, c_2:

$$\sigma\left(\frac{1}{\Delta t \kappa_\Delta} M^{1/2} G_b^{-T} M G_b^{-1} M^{1/2}\right) \subset \frac{1}{\Delta t \kappa_\Delta}[c_1 h^2, c_2].$$

Second (isotropic) term:

$$\sigma\left(\frac{\kappa_\perp}{\kappa_\Delta} M^{1/2} G_b^{-T} L G_b^{-1} M^{1/2}\right) \subset \left(0, \frac{\kappa_\perp c_3}{\kappa_\Delta h^2}\right],$$

$$\sigma\left((\sqrt{\kappa_\Delta} G_b^T)^{-1} S_{22}\right) \subset \left(1, 1 + \frac{\kappa_\perp c_3}{\kappa_\Delta h^2} + \frac{c_2}{\Delta t \kappa_\Delta}\right].$$

Spectral analysis of Schur complement

Eigenvalues computed in practice via Lanczos:

Δt	$\kappa_{\parallel}/\kappa_{\perp}$	2D			3D		
10^{-3}	10^3	7.8e0	4.7e0	4.3e0	6.6e2	4.0e2	3.4e2
	10^6	7.8e-3	4.7e-3	4.3e-3	6.6e-1	4.0e-1	3.4e-1
	10^9	7.8e-6	4.7e-6	4.3e-6	6.6e-4	4.0e-4	3.4e-4
10^{-2}	10^3	8.0e-1	1.5e0	3.7e0	6.6e1	1.1e2	2.8e2
	10^6	8.0e-4	1.5e-3	3.7e-3	6.6e-2	1.1e-1	2.8e-1
	10^9	8.0e-7	1.5e-6	3.7e-6	6.6e-5	1.1e-4	2.8e-4

Table: Largest eigenvalues of error propagation, $(\sqrt{\kappa_\Delta} G_b^T)^{-1} S_{22} - I$. The three values for each given anisotropy ratio correspond to three successive spatial refinement levels.

Results

- Analagous problem as DG convergence study, with open field lines so advection is invertible.
- Block preconditioned FGMRES, outer relative tolerance 10^{-8}.
- Inner AIR tolerance $\texttt{min}\{10^{-3}, 10^{-3}/\|\boldsymbol{b}\|\}$, where $\boldsymbol{b}$ is current right-hand side.
  - Effectively absolute *and* relative tolerance.
  - If $(\Delta t \kappa_\Delta)^{-1}$ or $\kappa_\perp/\kappa_\Delta$ is not $\ll 1$, right-hand side provided to second AIR solve can be very large, e.g., $\mathcal{O}(10^4)$. Then, relative tolerance 10^{-3} doesn't even lead to residual < 1 in norm, and outer iteration fails to converge.

Results

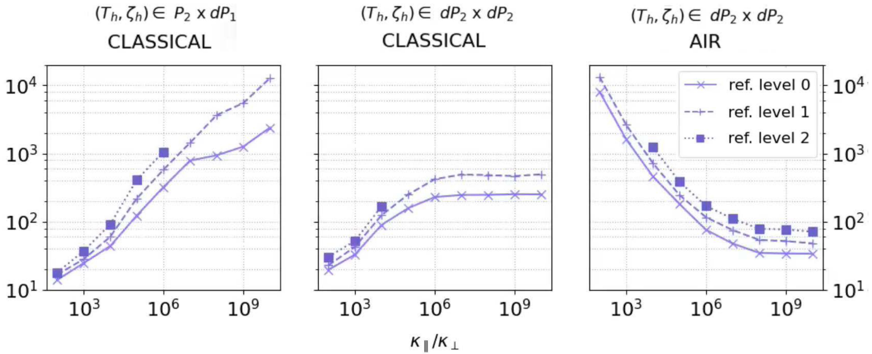

Figure: Average total inner iteration counts per time step. Left column: mixed CG, classical AMG. Center column: mixed DG, classical AMG. Right column: mixed DG, AIR.

Results

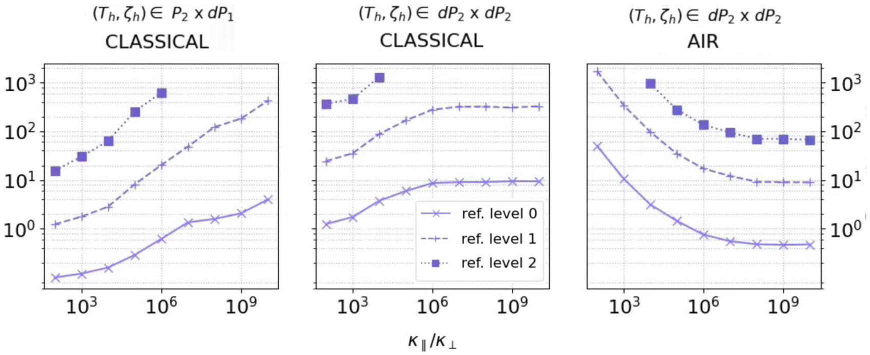

Figure: Average wall-clock times in seconds per time step. Left column: mixed CG, classical AMG. Center column: mixed DG, classical AMG. Right column: mixed DG, AIR.

Table of Contents

Difficulties with closed field lines

- Advection operators are no longer invertible (recall, no time derivative on advection term) $\implies$ cannot use open field lines approach directly.
- In one step, information traverses a closed field line *many* times.
- Will have closed field lines in most/all realistic problems.

Difficulties with closed field lines

- Advection operators are no longer invertible (recall, no time derivative on advection term) $\Longrightarrow$ cannot use open field lines approach directly.
- In one step, information traverses a closed field line *many* times.
- Will have closed field lines in most/all realistic problems.

Idea: keep reordered system

$$\begin{pmatrix} -\sqrt{\kappa_\Delta} G_b & M \\ \frac{1}{\Delta t} M + \kappa_\perp L & \sqrt{\kappa_\Delta} G_b^T \end{pmatrix} \begin{pmatrix} T^{n+1} \\ \zeta^{n+1} \end{pmatrix} = \begin{pmatrix} F_\zeta \\ F_T \end{pmatrix}.$$

and apply AIR all at once to this system.

DG Tokamak test case

	AMG iters		Rel accuracy	
ref level	CG2/DG1	DG2-DG2	CG2/DG1	DG2-DG2
0	438	145	0.13	0.1
1	2263	265	0.09	0.02
2	6312	380	0.06	0.01

Table: Two toroidal planes and physical κ values, AMG iters and accuracy shown for three poloidal ref levels.

Conclusions

Review:

- Diffusion in magnetic confinement fusion is extremely anisotropic in the direction of field lines.
- Rewrote diffusion system based on directional gradients, apply discretization and solver techniques developed for advection.
- Orders of magnitude decrease in error and solve wallclock time vs. traditional/existing methods.

Conclusions

Review:

- Diffusion in magnetic confinement fusion is extremely anisotropic in the direction of field lines.
- Rewrote diffusion system based on directional gradients, apply discretization and solver techniques developed for advection.
- Orders of magnitude decrease in error and solve wallclock time vs. traditional/existing methods.

Next steps:

- Incorporate into larger MHD simulations.
- Better solvers for closed field lines or mixed regimes.
- Other extremely anisotropic equations??

Thank you!

Papers:

[1] T. A. Manteuffel, S. Münzenmaier, J. Ruge, and B. S. Southworth. Nonsymmetric reduction-based algebraic multigrid.

[2] T. A. Manteuffel, J. Ruge, and B. S. Southworth. Nonsymmetric algebraic multigrid based on local approximate ideal restriction (ℓAIR).

[3] B. S. Southworth, A. A. Sivas, and S. Rhebergen. On fixed-point, Krylov, and block preconditioners for nonsymmetric problems.

[4] G. A. Wimmer, B. S. Southworth, T. J. Gregory, and X Tang. A fast algebraic multigrid solver and accurate discretization for highly anisotropic heat flux I: open field lines.

[5] G. A. Wimmer, B. S. Southworth, and X Tang. A fast algebraic multigrid solver and accurate discretization for highly anisotropic heat flux II: closed field lines and continuous elements (*in preparation*).